

EXPERIMENTAL AND MODELING STUDIES OF BORON INJECTION AND DEPOSITION IN SUPPORT OF ITER

¹F. EFFENBERG, ¹A. BORTOLON, ²K. SCHMID, ¹F. NESPOLI, ¹J.A. SNIPES, ³T. WAUTERS, ³A. LOARTE, ⁴T. ABRAMS, ⁵Y. FENG, ⁶H. FRERICHS, ⁷J.D. LORE, ¹R. MAINGI, ⁸D.L. RUDAKOV

¹Princeton Plasma Physics Laboratory, Princeton, NJ, United States of America

²Max Planck Institute of Plasma Physics, Garching, Germany

³ITER Organization, Saint-Paul-lès-Durance, France

⁴General Atomics, San Diego, CA, United States of America

⁵Max Planck Institute of Plasma Physics, Greifswald, Germany

⁶University of Wisconsin, Madison, WI, United States of America

⁷Oak Ridge National Laboratory, Oak Ridge, TN, United States of America

⁸University of California - San Diego, La Jolla, CA, United States of America

Email: feffenbe@pppl.gov

Integrated modeling of boron (B) powder injection for real-time wall conditioning in the DIII-D tokamak, combined with Laser-Induced Breakdown Spectroscopy (LIBS), reveals a uniform toroidal B distribution on the divertor and poloidally non-uniform deposition on the wall, accumulating near the outer strike point. Simulations predict the formation of boron-rich coatings with B concentrations exceeding 35% in localized regions on the divertor. These coatings, typically growing at rates of ~ 0.9 nm/s during material injection using the impurity powder dropper (IPD) [1], are shown to be driven by recycling and redeposition processes, closely aligning with experimentally measured surface compositions. The integrated modeling effectively captures the broad coverage and conditioning of DIII-D plasma-facing components (PFCs), providing detailed insight into transport and deposition dynamics. Furthermore, it informs the design of a solid boron injector for ITER [2, 3] and other fusion devices to mitigate high-Z impurity contamination and support high-performance plasma operations.

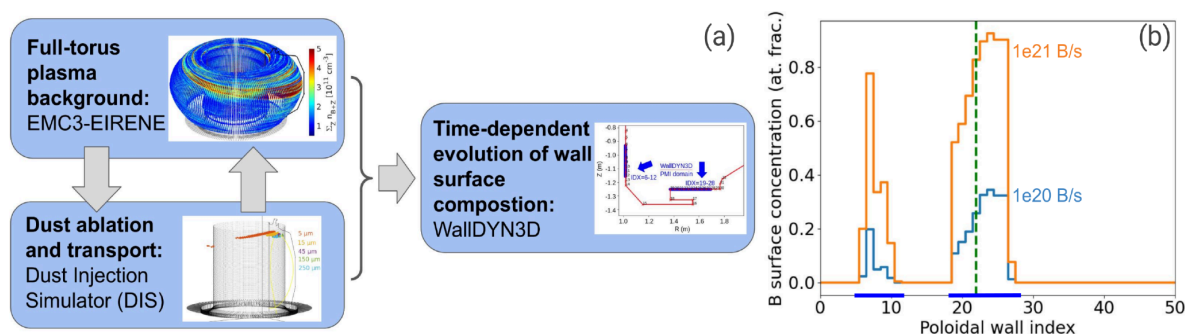


Figure 1. (a) Integrated modeling workflow: EMC3-EIRENE provides full-torus plasma background and fluid impurity transport modeling, the Dust Injection Simulator (DIS) simulates dust ablation and transport, and WallDYN3D calculates the dynamic mixed-material surface composition. (b) Final boron surface concentrations featuring peaks on the lower DIII-D divertor targets for both low and high B powder injection rates. The X-axis ('poloidal wall index') represents wall elements in the poloidal plane (see Fig. 1(a) and compare to Fig. 2(b)).

The integrated workflow combining EMC3-EIRENE, the Dust Injection Simulator (DIS), and WallDYN3D outlined in Fig. 1(a) was developed to simulate boron transport, deposition, and recycling under conditions relevant to real-time wall conditioning in DIII-D and potentially for in-situ coating in ITER [4]. The DIII-D simulations covered boron injection rates ranging from 1–10 mg/s, corresponding to atomic boron fluxes of 10^{20} – 10^{21} B/s, and were applied to a representative L-mode plasma scenario used for real-time wall conditioning. WallDYN3D modeling, incorporating erosion and redeposition processes, demonstrated a notable reduction in the in/outboard asymmetry of B fluxes, resulting in higher B concentrations on the outer divertor under steady-state conditions compared to the initial (or non-recycling) deposition. The modeling indicates that kinetic treatment of transport and recycling-driven redeposition significantly enhances the symmetry of B layer distributions compared to the initial (or non-recycling) deposition. The surface composition varied significantly with injection rates. At 10^{20} B/s, boron surface concentrations stabilized at $\sim 35\%$, with

the remaining ~65% accounted for by carbon, balancing the B-C mixed material surfaces as shown for B in Fig 1(b). In contrast, higher injection rates of 10^{21} B/s in the same plasma scenario resulted in near-pure boron layers with area densities reaching 3.6×10^{16} atoms/cm². The temporal evolution of boron deposition showed rapid redistribution from initial asymmetric profiles to quasi-symmetrical distributions due to enhanced recycling at higher injection rates.

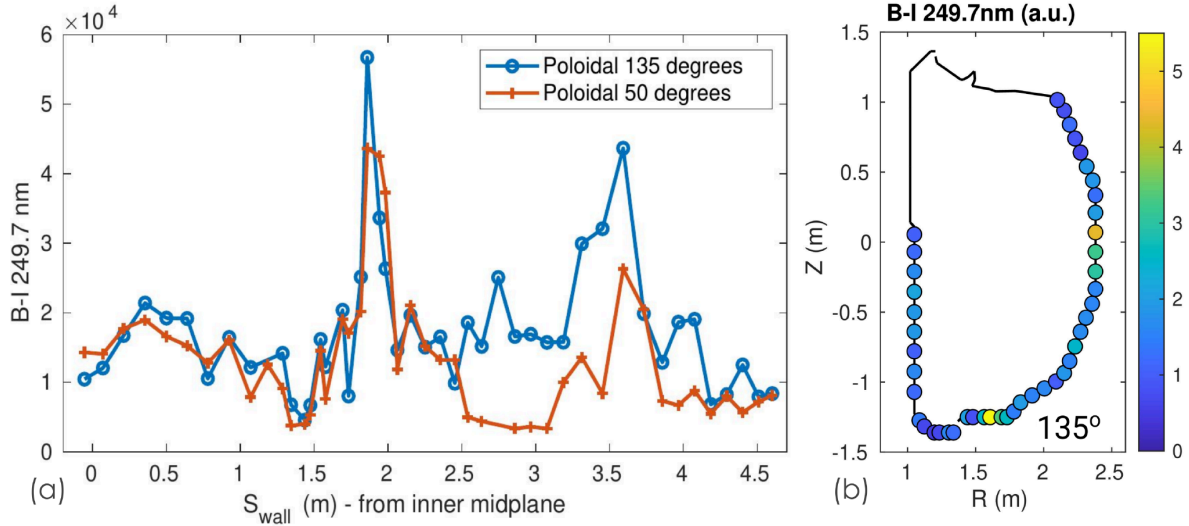


Figure 2: In-vessel mapping of DIII-D plasma-facing components using Laser-Induced Breakdown Spectroscopy (LIBS). (a) Poloidal scan of B I (249.7 nm) emission intensities at two toroidal angles (50° and 135°), showing the spatial distribution of boron on plasma-facing components near and far from the glow-discharge boronization anode. (b) Poloidal mapping at a toroidal angle of 135°, providing a detailed spatial representation of boron deposition.

Integrated modeling results were compared with high-resolution post-campaign LIBS measurements, mapping boron deposition across DIII-D PFCs. A total of 266 measurements spanned five toroidal and two poloidal arrays. The LIBS system, operating with a 1064 nm Nd:YAG laser at 20 Hz, ablated surface materials to depths of approximately 0.5 μm , capturing emissions in the 190–950 nm spectral range. Key elements identified included boron, lithium, carbon, oxygen, and deuterium. The LIBS spectra feature multiple characteristic boron and carbon lines, confirming mixed B-C layers on the PFCs. The poloidal B distributions, represented by B-I (249.7 nm), of two scans, one close to a glow-discharge boronization (GDB) anode (135°) and one distant (50°), are shown in Fig. 2. The highest B-I intensities were measured on the lower divertor (~1.86 m) in the same region as predicted by modeling for sole IPD B powder injection and at the outer midplane (~3.59 m), near the GDB anode (not included in the modeling).

This work combines advanced modeling with high-resolution experimental validation to provide critical insights into boron injection for real-time wall conditioning and coating. The integrated approach deepens the understanding of boron transport, deposition, and recycling dynamics, supporting the development of in-situ coating strategies for ITER during Q=10 operations [3] and enhancing the performance of future high-Z metallic fusion devices.

ACKNOWLEDGEMENTS

Work supported by DOE Award No. DE-AC02-09CH11466, DE-FC02-04ER54698, DE-SC0020357, and DE-AC05-00OR22725.

REFERENCES

- [1] A. Bortolon et al 2020 Nucl. Fusion 60 126010
- [2] A. Loarte et al 2024 ITER Technical Report ITR-24-004
- [3] J.A. Snipes et al 2024 Nucl. Mat. Energy 41 101809
- [4] F. Effenberg et al 2025 Nucl. Mat. Energy 42 101832